Cell, Vol. 105, 221–232, April 20, 2001, Copyright ©2001 by Cell Press

The CaMKII UNC-43 Activates the MAPKKK NSY-1 to Execute a Lateral Signaling Decision Required for Asymmetric Olfactory Neuron Fates

Alvaro Sagasti,* Naoki Hisamoto,† Junko Hyodo,† Miho Tanaka-Hino,† Kunihiro Matsumoto,† and Cornelia I. Bargmann*‡

*Howard Hughes Medical Institute
Programs in Developmental Biology, Neuroscience, and Genetics
Department of Anatomy and Department of Biochemistry and Biophysics
The University of California, San Francisco
San Francisco, California 94143
†Department of Molecular Biology
Graduate School of Science
Nagoya University and CREST, Japan Science and Technology Corporation
Chikusa-ku, Nagoya
464-8602 Japan

Summary

A stochastic cell fate decision mediated by axon contact and calcium signaling causes one of the two bilaterally symmetric AWC neurons, either AWCL or AWCR, to express the candidate olfactory receptor *str-2*. *nsy-1* mutants express *str-2* in both neurons, disrupting AWC asymmetry. *nsy-1* encodes a homolog of the human MAP kinase kinase kinase (MAPKKK) ASK1, an activator of JNK and p38 kinases. Based on genetic epistasis analysis, *nsy-1* appears to act downstream of the CaMKII *unc-43*, and NSY-1 associates with UNC-43, suggesting that UNC-43/CaMKII activates the NSY-1 MAP kinase cassette. Mosaic analysis demonstrates that UNC-43 and NSY-1 act primarily in a cell-autonomous execution step that represses *str-2* expression in one AWC cell, downstream of the initial lateral signaling pathway that coordinates the fates of the two cells.

Introduction

Olfactory neurons fall into many distinct classes that can be distinguished by the expression of different odorant receptor genes. This diversity is observed even in the simple nervous system of the nematode *C. elegans*, which includes at least fourteen functionally different classes of chemosensory neurons (White et al., 1986). In general, the chemosensory neurons of *C. elegans* exhibit bilateral symmetry, with pairs of similar neurons located on the left and right sides of the animal. A further level of diversity is achieved in the AWC olfactory neuron pair through a cell interaction between the two AWC cells (AWCL and AWCR). The candidate olfactory receptor gene *str-2* is expressed asymmetrically and stochastically in only one of the two AWC neurons: half of a population of animals expresses a *str-2*::GFP reporter gene in AWCR and half expresses it in AWCL (Troemel et al., 1999). Asymmetry between the two AWC neurons enables the animal to detect more odors and discriminate between them in complex environments (Wes and Bargmann, 2001). The AWC cells can be defined as AWC^{ON} and AWC^{OFF} based on their pattern of *str-2::GFP* expression. If the precursor to one AWC neuron is killed early in development, the surviving neuron always becomes AWC^{OFF}, suggesting that the two cells communicate to establish the AWC^{ON} fate. In mutants in which the AWC axons terminate prematurely, both neurons become AWC^{OFF}, suggesting that axon contact between the AWC neurons is required for cell communication.

The cell interaction that determines AWC asymmetry is reminiscent of lateral signaling, but appears to use a unique signaling pathway that is not affected by mutations in the *C. elegans* Notch genes *lin-12* and *glp-1* (Kimble and Simpson, 1997). A screen for *N*euronal *sy*mmetry (Nsy) mutants that express *str-2*::GFP in both AWC cells yielded mutations in three genes involved in calcium signaling (Troemel et al., 1999). *unc-2* and *unc-36* encode *C. elegans* homologs of subunits of an N/P-type voltage-gated calcium channel (Lee et al., 1997; Schafer and Kenyon, 1995) and *unc-43* encodes the single *C. elegans* homolog of the calcium/calmodulin-dependent serine/threonine protein kinase CaMKII (Reiner et al., 1999). These observations suggest that the interaction between the AWC neurons inhibits the activity of the calcium channel-CaMKII signaling pathway, which represses *str-2* expression in one cell. The decision is made early in development and is stabilized by a separate cGMP-dependent maintenance pathway.

The screen for mutants with two AWC^{ON} neurons also yielded three *nsy* genes that map to novel loci. We show here that the AWC asymmetry gene *nsy-1* encodes a protein homologous to a human MAPKKK, the apoptosis signal–regulating kinase ASK1. ASK1 activates the JNK and p38 MAP kinases in mammalian cells and induces cell death in response to TNFα (Ichijo et al., 1997). Our results suggest that the ASK1 JNK/p38 pathway is a central component of the AWC cell fate decision. *nsy-1* is genetically downstream of the CaMKII homolog *unc-43* in the regulation of AWC asymmetry. Mosaic analysis reveals that CaMKII acts in a strictly cell-autonomous manner in AWC^{OFF} to execute the cell fate decision made by the AWC lateral signaling pathway. NSY-1 also acts primarily to execute cell fate in AWC^{OFF} but may play an additional minor, *unc-43*-independent role in coordinating the fates of the two AWC neurons. The related functions of the CaMKII *unc-43* and the MAPKKK *nsy-1* in the execution of AWC cell fate reveal a novel link between calcium signaling and a MAPK signaling cassette, suggesting a strategy by which neurons use calcium signals to achieve an all-or-none developmental response.

Results

NSY-1 Is a Homolog of the Human MAPKKK ASK1

Mutations in the *nsy-1*, *nsy-2*, and *nsy-3* genes cause *str-2*::GFP to be expressed in both AWC neurons (2

‡To whom correspondence should be addressed (e-mail: cori@itsa.ucsf.edu).

AWC^{ON}) (Troemel et al., 1999). We mapped the *nsy-1* gene and cloned it by transgene rescue of the mutant *str-2*::GFP expression phenotype. A clone that contained only the complete open reading frame for the gene F59A6.1 rescued the *nsy-1(ky397)* mutant phenotype (see Experimental Procedures), and RNA interference of the F59A6.1 gene caused a mild 2 AWC^{ON} phenotype in wild-type animals (data not shown). Nonsense mutations in F59A6.1 were identified in all three *nsy-1* alleles (Figure 1A and below). We conclude that the *nsy-1* gene corresponds to the open reading frame F59A6.1.

nsy-1 encodes a homolog of the human MAP kinase kinase kinase (MAPKKK) ASK1 (Ichijo et al., 1997). We generated a full-length cDNA for *nsy-1* and found that the two proteins are 44% identical over 884 amino acids and 63% identical in their kinase domains (Figure 1A). It is likely that *nsy-1* and ASK1 are orthologs (Plowman et al., 1999). The mutations in *nsy-1(ky400)* and *nsy-1(ky542)* result in premature stop codons just before the kinase domain, and the mutation in *nsy-1(ky397)* creates a premature stop codon after the kinase domain (Figure 1A). All of these alleles have similar *str-2*::GFP misexpression phenotypes and are likely to represent null alleles of the *nsy-1* gene.

MAPKKKs are a conserved family of serine/threonine kinases that play important developmental and physiological roles in eukaryotic cells (Garrington and Johnson, 1999). These kinases phosphorylate MAP kinase kinases (MAPKK), which in turn phosphorylate and activate MAP kinases (MAPK). ASK1 has been shown to phosphorylate the MAPKK MKK6, and to activate the JNK and p38 MAPKs, but not the ERK MAPK (Ichijo et al., 1997). To confirm that NSY-1 and ASK1 have similar functions, we expressed NSY-1 in mammalian HEK 293 cells. A wild-type form of NSY-1 efficiently phosphorylated MKK6 in vitro, but a kinase-negative form did not (Figure 1B). NSY-1 expression in mammalian cells also stimulated phosphorylation of endogenous p38 kinases (Figure 1B). These results suggest that NSY-1 functions as a MAPKKK with similar specificity to the human protein ASK1.

NSY-1 and UNC-43 Function in the AWC Neurons to Regulate AWC Cell Fate

To determine where NSY-1 is expressed, we made fusions between the *nsy-1* gene and GFP and examined their expression patterns in transgenic animals (Chalfie et al., 1994). A GFP fusion gene containing 10 kb of sequence upstream of the *nsy-1* translational start site was expressed in the intestine, hypodermis, rectal gland cells, and neurons, including both AWC neurons (Figures 2A and 2B). A shorter transcriptional GFP fusion gene with 5 kb of upstream sequence, and a translation fusion of GFP to the entire NSY-1 protein with 3.8 kb of upstream sequence, were expressed in many cells but not in the AWC neurons (data not shown). Full rescue of the *nsy-1* phenotype required more than 3.8 kb of upstream sequence, suggesting that expression of the gene in the AWC neurons was needed for rescue of a *nsy-1* mutant.

To ask whether NSY-1 expression in AWC is sufficient to rescue *nsy-1* mutants, we placed the *nsy-1* cDNA under the control of the *odr-3* promoter. This promoter drives strong expression in both AWC neurons, weak expression in the AWB neurons, and variable expression in AWA, ADF, and ASH neurons (Roayaie et al., 1998). AWA, AWB, ADF, and ASH do not make synaptic connections with AWC (White et al., 1986). The *odr-3::*NSY-1 transgene rescued the 2 AWC^{ON} asymmetry defect of *nsy-1* mutants and occasionally caused a gain-of-function (2 AWC^{OFF}) phenotype, supporting the hypothesis that NSY-1 acts in the AWC neurons to mediate AWC asymmetry (Table 1).

Since the CaMKII homolog *unc-43* has a similar phenotype to *nsy-1*, we asked whether it could also function in AWC neurons. An *unc-43* cDNA (Rongo and Kaplan, 1999) under the control of the *odr-3* promoter rescued the 2 AWC^{ON} *str-2*::GFP phenotype of an *unc-43* mutant and occasionally caused a gain-of-function (2 AWC^{OFF}) phenotype (Table 1), consistent with the possibility that *unc-43* acts in the AWC neurons. A gain-of-function *unc-43* cDNA (Rongo and Kaplan, 1999) under the control of the *odr-3* promoter also caused *str-2*::GFP to turn off in both AWC cells (2 AWC^{OFF}; Table 1).

Because the *odr-3* promoter is reproducibly expressed in both AWC and AWB neurons, it is possible that *nsy-1* and *unc-43* expression in AWB rescues AWC cell fate. To rule out this possibility, we examined mosaic animals that expressed *odr-3*::NSY-1 or *odr-3*::UNC-43 in the AWB neurons but not the AWC neurons. Mosaic animals arose through the random loss of extrachromosomal arrays containing both *odr-3*::NSY-1 (or *odr-3*::UNC-43) and the marker *odr-1*::RFP in a *nsy-1* (or *unc-43*) mutant background (see below and Experimental Procedures). *str-2*::GFP asymmetry was rescued when the arrays were present in AWC neurons, but not when they were present only in AWB neurons (see Experimental Procedures). The *odr-3*::UNC-43(GF) phenotype also correlated with expression in AWC. These results demonstrate that *str-2*::GFP asymmetry is most likely mediated by expression of *nsy-1* and *unc-43* in AWC. Since the *odr-3* promoter drives expression in both AWC cells, asymmetric expression of UNC-43 and NSY-1 is not necessary for asymmetric expression of *str-2*.

nsy-1 May Act Downstream of the CaMKII Homolog *unc-43*

To characterize the roles of the *nsy* genes in AWC asymmetry, we analyzed epistasis relationships between the novel *nsy* genes and genes that affect axon guidance, calcium signaling, and olfactory cGMP signaling. Two AWC^{ON} neurons are present in *nsy* mutants, loss-of-function mutations in the calcium channel subunits *unc-2* and *unc-36*, and null mutants in the CaMKII *unc-43*. Two AWC^{OFF} neurons are present in gain-of-function *unc-43* mutants (*unc-43(gf)*) and in mutants that cause early axon termination, like *unc-76*. *unc-76* and other axon guidance mutants presumably block primary signaling between the two AWC axons. Two AWC^{OFF} neurons are also present in mutants for the *odr-1* transmembrane guanylyl cyclase and other olfactory cGMP signaling molecules that are essential for maintenance of *str-2* expression. Previous epistasis analysis placed the axon guidance gene *unc-76* upstream of the calcium signaling genes, and the guanylyl cyclase *odr-1* downstream of all other genes that affect AWC asymmetry (Troemel et al., 1999).

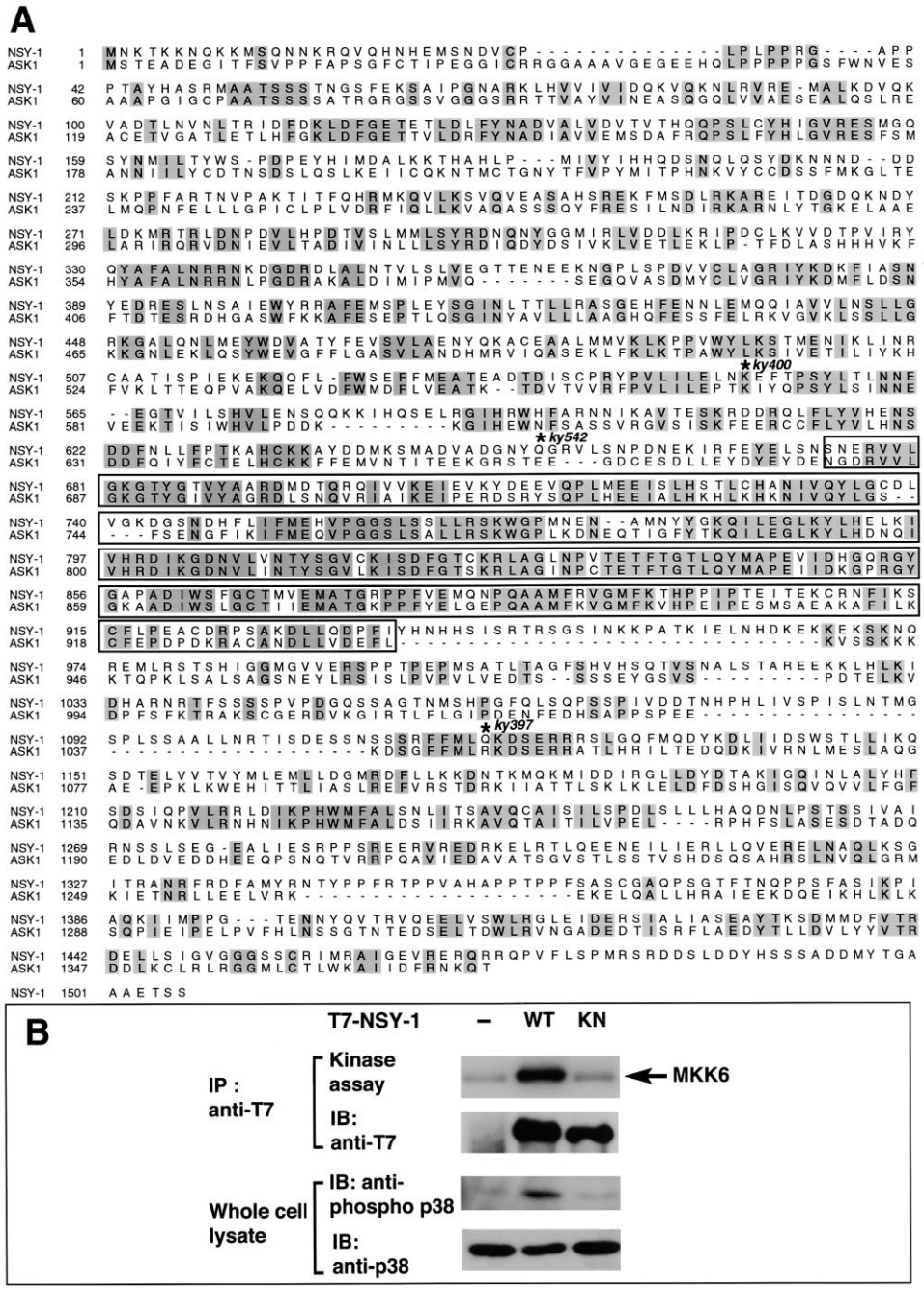

Figure 1. *nsy-1* Encodes a MAPKKK Related to the Human Protein ASK1

(A) ClustalW alignment of the NSY-1 and ASK-1 protein sequences. Shading indicates identical residues. The kinase domain is boxed. Residues that were mutated to stop codons in the three *nsy-1* alleles are indicated by an asterisk and allele number above the mutant residue.

(B) NSY-1 has MAPKKK activity in mammalian cells. Human embryonic 293 cells were transiently transfected with a control vector (−), NSY-1 tagged with a T7 epitope (WT), and a T7-tagged catalytically inactive form of NSY-1, in which Lys-703 in the ATP binding domain was replaced by methionine (KN). The complexes immunoprecipitated (IP) with anti-T7 were tested in in vitro kinase reactions with bacterially expressed MKK6 as a substrate (top panel). The immunoprecipitates were also immunoblotted with anti-T7 (second panel). To determine whether NSY-1 is able to activate a mammalian p38 MAPK pathway in vivo, whole-cell extracts were immunoblotted with anti-phospho-p38 (third panel), an antibody that specifically recognizes the dually phosphorylated active form of p38, and anti-p38 (bottom panel). NSY-1 efficiently phosphorylated MKK6 in vitro and activated p38 in cells, whereas catalytically inactive NSY-1(KN) did not.

We found that *nsy-3* (2 AWC^{ON}) was epistatic to the *unc-76* axon guidance mutant (2 AWC^{OFF}), whereas a gain-of-function mutant in the CaMKII *unc-43* (2 AWC^{OFF}) was epistatic to *nsy-3* (Table 2). These results suggest that *nsy-3* acts upstream of *unc-43*. Both *nsy-1* and *nsy-2* (2 AWC^{ON}) were epistatic to *unc-76* and *unc-43(gf)* (Table 2). These results suggest that *nsy-1* and *nsy-2* act downstream of or in parallel to *unc-43*. The *odr-1*

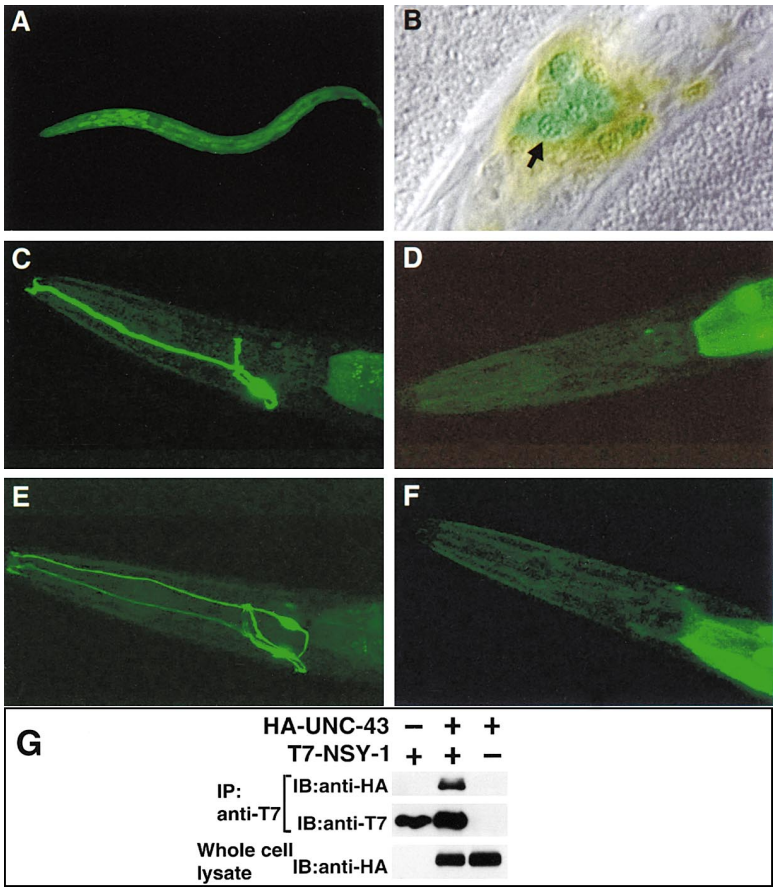

Figure 2. *nsy-1* Is Expressed in the AWC Neurons and May Act Downstream of *unc-43*/CaMKII

(A and B) A *nsy-1*::GFP transgene with ~10 kb of *nsy-1* upstream sequence was expressed in many cells, including AWC. (A) A confocal projection of an L1 larval stage animal with wide expression of *nsy-1*::GFP. (B) Merged *nsy-1::GFP* and Nomarski images of an L1 animal. An arrow indicates AWC.

(C–F) Animals bearing an integrated *str-2*::GFP reporter. Fluorescence posterior to the head is gut autofluorescence or gut expression of the transgene marker *elt-2*::GFP. (C) Wild-type animals expressed *str-2*::GFP in one AWC neuron. (D) Animals expressing *odr-3*::NSY-1(GF) did not express *str-2*::GFP in either AWC neuron. (E) An *unc-43* loss-of-function mutation caused *str-2*::GFP expression in both AWC neurons. (F) An *unc-43* loss-of-function mutant expressing *odr-3*::NSY-1(GF) did not express *str-2*::GFP in either AWC neuron. The dorsally-located, dim-staining cells in (D) and (F) are the ASI neurons, where *str-2*::GFP is sometimes weakly expressed. Dorsal is up and anterior is to the left in all panels.

(G) Association between UNC-43 and NSY-1 in mammalian cells. Human embryonic 293 cells were transfected with a control vector (–); an HA-tagged, calcium-independent, activated form of UNC-43, HA-UNC-43(T284D); and a catalytically inactive, T7-tagged form of NSY-1, T7-NSY-1(K703M). Cell lysates were immunoprecipitated (IP) with anti-T7 antisera. Immunoprecipitates were immunoblotted (IB) with anti-HA (top panel) and anti-T7 (middle panel); UNC-43 was present in the NSY-1 immunoprecipitate (top panel). Whole-cell extracts were also immunoblotted with anti-HA (bottom panel).

guanylyl cyclase mutant (2 AWC^{OFF}) was epistatic to *nsy-1*, *nsy-2*, and *nsy-3*, as predicted by its later role in *str-2* maintenance (Table 2).

As an additional tool for epistasis analysis, a gain-of-function *nsy-1* allele *(nsy-1(gf))* was made by deleting the N-terminal 640 amino acids encoded by the cDNA. The analogous mutation in the NSY-1 mammalian homolog ASK1 creates a gain-of-function protein (Saitoh et al., 1998). A *nsy-1(gf)* transgene under the control of the *odr-3* promoter conferred a 2 AWC^{OFF} phenotype, the opposite phenotype of *nsy-1(lf)* (Table 1 and Figure 2D). The AWC marker *odr-1::*RFP was expressed normally in *nsy-1(gf)* strains, confirming that the AWC neurons were viable and properly specified. Thus, like *unc-43*, *nsy-1* can act as a switch for AWC cell fates.

To determine whether *nsy-1* acts downstream of or in parallel to *unc-43*, the *nsy-1(gf)* transgene (2 AWC^{OFF}) was crossed into an *unc-43(lf)* mutant (2 AWC^{ON}). The *unc-43(n1186lf)* allele used in these experiments contains an early stop codon in the kinase domain and is a predicted null mutation (Reiner et al., 1999). Just as *nsy-1(lf)* is epistatic to *unc-43(gf)*, the *nsy-1(gf)* phenotype was epistatic to the *unc-43(lf)* phenotype (Figures 2C–2F and Table 2). If *nsy-1* and *unc-43* were required in parallel to repress *str-2*::GFP expression, then loss-of-function mutants would be expected to be epistatic to gain-of-function mutants in both cases. These epistasis results are therefore consistent with *nsy-1* acting downstream of *unc-43* in a linear genetic pathway to regulate AWC asymmetry.

Given the genetic similarities between *nsy-1* and *unc-43* in the AWC cell fate decision, it is possible that UNC-43 interacts with NSY-1. We tested whether NSY-1 and UNC-43 interact physically by expressing a catalytically inactive form of NSY-1, tagged with a T7 epitope, and a constitutively active form of UNC-43, tagged with HA, in mammalian HEK 293 cells. Immunoprecipitation with anti-T7 antibodies brought down both UNC-43 and NSY-1 (Figure 2G). Similar experiments with a wild-type UNC-43 protein and a kinase-dead UNC-43 protein indicated that all of these forms of UNC-43 interact with NSY-1 (data not shown).

Dissecting the Circuitry of AWC Signaling: *unc-43* Executes the AWC^{OFF} Cell Fate in a Cell-Autonomous Fashion and Does Not Influence the Fate of the AWC^{ON} Cell

Since the two AWC neurons signal to each other, *unc-43* and *nsy-1* could act either in the AWC^{OFF} cell to repress *str-2* expression cell autonomously, or in the AWC^{ON} cell to send a nonautonomous signal to the contralateral AWC^{OFF} cell. Previous experiments suggested that the calcium signaling pathway acts at least partly in AWC^{OFF}. When one AWC precursor cell is killed in a

Table 1. Targeted Gene Expression and Mosaic Analysis

Genetic Background	Transgene	2 AWC^{OFF} (%)	1 AWC^{OFF}/ 1 AWC^{ON} (%)	2 AWC^{ON} (%)	n
		Transgene expressed in both AWC cells[1]			
unc-43(n1186)	*odr-3*::UNC-43 a	16	55	29	778
	odr-3::UNC-43 b	12	68	20	634
Wild-type	*odr-3*::UNC-43(GF) a	87	13	0	447
	odr-3::UNC-43(GF) b	86	12	1	626
	odr-3::UNC-43(GF) c	85	14	0	240
nsy-1(n397)	*odr-3*::NSY-1 a	2	93	5	659
	odr-3::NSY-1 b	18	79	4	884
	odr-3::NSY-1 c	17	80	3	646
Wild-type	*odr-3*::NSY-1(GF) a	90	10	0	626
	odr-3::NSY-1(GF) b	95	4	1	536
	odr-3::NSY-1(GF) c	83	17	0	329
	odr-3::NSY-1(GF) d	91	9	0	862
	odr-3::NSY-1(GF) e	78	22	0	673

		Mosaic animals with one wild-type and one mutant AWC neuron[1]						
			1 AWC^{OFF}/1 AWC^{ON} (%)[3]				χ^2 analysis for execution model[2]	
		2 AWC^{OFF} (%)	Wildtype AWC^{ON}/ Mutant AWC^{OFF}	Wildtype AWC^{OFF}/ Mutant AWC^{ON}	2 AWC^{ON} (%)	n	χ^2	p
unc-43(n1186)	*odr-3*::UNC-43 a	0	3	46	51	71	0.53	0.2–0.5
	odr-3::UNC-43 b	3	7	44	47	146	1.4	0.2–0.5
Wild-type	*odr-3*::UNC-43(GF) a	34	54	11	1	119	5.72	0.2–0.5
	odr-3::UNC-43(GF) b	46	49	5	0	74	0.13	>0.9
	odr-3::UNC-43(GF) c	47	47	6	0	104	0.79	0.5–0.9
nsy-1(ky397)	*odr-3*::NSY-1 a	0	3	66	32	79	11.4	<0.001
	odr-3::NSY-1 b	3	10	65	22	124	14.9	<0.001
	odr-3::NSY-1 c	0	5	65	30	82	3.63	0.05–0.20
Wild-type	*odr-3*::NSY-1(GF) a	43	51	6	0	104	0.30	0.5–0.9
	odr-3::NSY-1(GF) b	78	19	2	2	63	23.6	<0.001
	odr-3::NSY-1(GF) c	44	47	9	0	96	0.42	0.5–0.9
	odr-3::NSY-1(GF) d	54	37	9	0	180	17.10	<0.001
	odr-3::NSY-1(GF) e	38	42	20	0	98	8.7	0.01–0.05

[1]Results for single mutants are reported in Table 2. For *unc-43(lf)* analysis, an *odr-3*::UNC-43 transgene was introduced into *unc-43(n1186)* mutants. For *unc-43(gf)* analysis, an *odr-3*::UNC-43(GF) transgene was introduced into wild-type animals. Similarly, for *nsy-1(lf)* analysis, an *odr-3*::NSY-1 transgene was introduced into *nsy-1(ky397)* mutants and for *nsy-1(gf)* analysis, an *odr-3*::NSY-1(GF) transgene was introduced into wild-type animals. An *odr-1*::RFP transgene was used to identify AWC cells which retained the array. Upper table reports results for animals which retained the array in both AWC cells (2 RFP+ cells). Lower table reports results for mosaic animals which retained the array in only one AWC cell (1 RFP− and 1 RFP+ cell). Lower case letters designate independent lines.

[2]Statistical analysis was also used to test a lateral interaction model. In all cases, $p < 0.001$, excluding the model.

[3]For LF mosaic analysis, the wild-type cell was RFP+, and the mutant cell was RFP−. For GF mosaics, the wild-type cell was RFP− and the GF mutant was RFP+.

wild-type background, the surviving AWC cell takes on the AWC^{OFF} fate. However, killing one AWC precursor in the 2 AWC^{ON} mutant *unc-36* leaves a surviving AWC^{ON} cell, suggesting that *unc-36* can act autonomously in a single AWC cell (Troemel et al., 1999). Similarly, the axon termination mutant *unc-76* has a 2 AWC^{OFF} phenotype, presumably because the AWC axons do not make contact and signal to each other. Double mutants between 2 AWC^{ON} Nsy mutants and *unc-76* have a 2 AWC^{ON} phenotype (Table 2; Troemel et al., 1999), suggesting that the Nsy genes are required cell autonomously in AWC^{OFF}, even in the absence of direct cell contact. A more definitive mosaic analysis experiment confirmed that *unc-43* and *nsy-1* are required cell autonomously for the AWC^{OFF} fate (Table 1 and below).

To understand the roles of *unc-43* and *nsy-1* in the signaling circuitry that determines AWC cell fates, it is important to ask whether they have a nonautonomous role in addition to their autonomous one. Since the AWC neurons communicate to coordinate the two AWC cell fates, the AWC cell fate determination pathway can be broken down into two components: a nonautonomous cell interaction pathway that coordinates the fates of the AWC^{ON} and AWC^{OFF} cells and a strictly cell-autonomous pathway that executes the fate determined by the first part of the pathway (Figure 3A). By analogy with the Notch/Delta lateral signaling pathway, the first part of the AWC pathway may include feedback that amplifies small differences in the signaling properties of the two AWC neurons (Kimble and Simpson, 1997). *unc-43* and *nsy-1* could function in a solely cell-autonomous manner to repress *str-2* expression downstream of the cell inter-

Table 2. Epistasis Analysis

Strain	Cells expressing *str-2*::GFP (%)			n
	2 AWC^{OFF}	1 AWC^{ON}/1 AWC^{OFF}	2 AWC^{ON}	
Single mutants				
unc-76(e911)[1]	43	57	0	114
odr-1(n1933)[1]	100	0	0	150
unc-43(n1186lf)[1]	3	5	92	101
unc-43(n498gf)[1]	80	20	0	133
nsy-1(ky397)[1]	0	0	100	34
nsy-2(ky388)[1]	0	32	68	62
nsy-3(ky389)[1]	0	4	96	107
odr-3::NSY-1(GF) transgene[2]	81	19	0	53
Double mutants				
nsy-1; unc-76	0	12	88	85
nsy-1; unc-43(n498gf)	2	5	93	59
nsy-1; odr-1	98	2	0	58
nsy-2, unc-76	2	24	75	170
nsy-2; unc-43(n498gf)	0	39	61	75
nsy-2; odr-1	100	0	0	75
nsy-3; unc-76	0	12	88	49
nsy-3; unc-43(n498gf)	97	3	0	33
nsy-3; odr-1	100	0	0	40
unc-43(n1186lf); odr-3::NSY-1(GF) transgene[2]	76	15	9	102

[1]These data are reproduced from Troemel et al., 1999.
[2]Results of two transgenic lines were combined. Both lines exhibited similar proportions of phenotypic classes.

action machinery, or they could function during feedback and thus act both autonomously and nonautonomously to coordinate the fates of the two AWC neurons.

The cell-autonomous and nonautonomous functions of *unc-43* and *nsy-1* can be defined in mosaic animals containing one wild-type and one mutant AWC neuron. Figures 3B and 3C diagram the distinct predictions for mosaics with either loss-of-function or gain-of-function mutant genes, depending on whether *nsy-1* and *unc-43* act to coordinate the fates of the two AWC cells through cell interaction and feedback, or only to execute the AWC^{OFF} fate. For example, if *unc-43* acted during AWC cell interaction and feedback, *unc-43(lf)* mosaic animals would always have exactly one AWC^{ON} and one AWC^{OFF} cell. The *unc-43* mutant cell would always be AWC^{ON} because the AWC^{OFF} execution pathway could not be activated, and the wild-type cell would always be AWC^{OFF}, the default state, because the *unc-43* mutant cell would not participate in interaction and feedback (Figure 3B). This model predicts both a cell-autonomous and a nonautonomous function for *unc-43*, as is observed for the Notch homolog *lin-12* in the AC/VU decision (Seydoux and Greenwald, 1989; see Discussion). Alternatively, if *unc-43* were only required to execute the AWC^{OFF} fate, the mutant cell would always be AWC^{ON} because of the defect in execution, but the wild-type cell would now adopt the AWC^{ON} or AWC^{OFF} fates with equal frequencies because the initial communication between the two cells occurred normally (Figure 3B). For gain-of-function mosaics, if *unc-43* acted in cell interaction and feedback, the *unc-43(gf)* cell would always be AWC^{OFF} and the wild-type cell would always be AWC^{ON}. However, if *unc-43* acted only to execute the AWC^{OFF} fate, the *unc-43(gf)* cell would again always be AWC^{OFF} but the wild-type cell would be AWC^{OFF} or AWC^{ON} with equal frequency (Figure 3C).

Mosaic analysis was conducted with *unc-43(lf)* animals bearing a transgenic extra-chromosomal array of *odr-3*::UNC-43 and *odr-1*::RFP. The *odr-1* promoter drives expression in the AWB and AWC neurons (Yu et al., 1997). Due to cosegregation of the genes in the extrachromosomal array, AWC neurons that retained the array were wild-type for *unc-43* (*unc-43*(+)) and expressed *odr-1*::RFP (RFP+), whereas AWC neurons that lost the array were *unc-43*(−) and RFP−. Mosaic animals with one RFP+ AWC neuron were identified in two transgenic lines. Internal controls were generated in each transgenic line by scoring animals that retained the array in both AWC cells (to determine the efficacy of the rescuing arrays) and animals that lost the array altogether (to determine the penetrance of the mutant phenotype). Animals that lost the array altogether displayed a high penetrance 2 AWC^{ON} *unc-43* phenotype (see Experimental Procedures). The results for mosaic animals and controls are presented in Table 1 and Figures 4A–4D. Both lines exhibited two major classes of mosaics (Table 1): animals in which *str-2*::GFP was only expressed in the mutant, non-RFP-expressing cell and animals in which both the mutant and wild-type cells expressed *str-2*::GFP. These are the two classes expected if *unc-43* were acting to execute the AWC^{OFF} cell fate, but not to coordinate the two AWC fates via cell interaction and feedback (Figure 3B). Statistical analysis of both lines, using the internal controls to generate predictions, was consistent with the model that *unc-43* acts to execute the AWC^{OFF} cell fate decision (Table 1).

Mosaic analysis was also performed with a wild-type strain bearing a transgenic extrachromosomal array of *odr-3*::UNC-43(GF) and *odr-1*::RFP. AWC neurons that retained the array were *unc-43(gf)* and RFP+, whereas AWC neurons that lost the array were *unc-43*(+) and RFP−. Mosaic animals with one RFP+ AWC neuron were identified in three transgenic lines, and internal controls were generated in each line. The results for

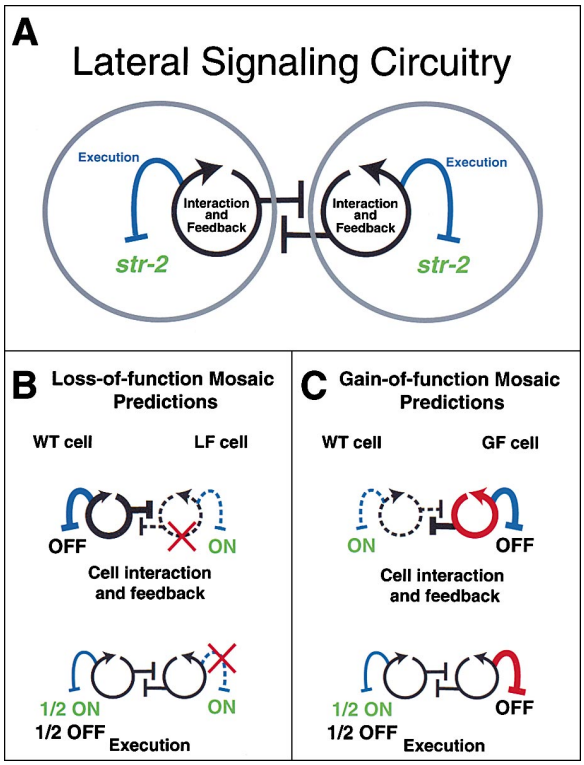

Figure 3. Mosaic Analysis Can Be Used to Analyze the Determination of AWC Fates

(A) Diagram of a hypothetical lateral signaling pathway. The lateral signaling circuitry can be divided into two components. The first component (black) consists of nonautonomous cell interaction with feedback, used by one cell to instruct the other to adopt the opposite fate. The second component (blue) is a pathway that executes the cell fate decision determined by the cell interaction. In the AWC^{OFF} cell, this pathway represses transcription of *str-2*.

(B) Loss-of-function mosaics with one wild-type and one mutant AWC cell can distinguish whether the *nsy-1* and *unc-43* genes function in cell interaction or in executing the AWC^{OFF} fate. A red "X" indicates the defect in a loss-of-function mutant.

(C) Gain-of-function mosaics with one wild-type and one *gf* mutant cell can also distinguish whether Nsy genes act in cell communication or execution. Red indicates the focus of a gain-of-function transgene. See text for detailed discussion of models. Dashed lines indicate an inactive pathway, thickened lines indicate an activated pathway, and unbroken, unthickened lines indicate a pathway with the potential to be active or inactive.

controls and mosaic animals are presented in Table 1 and Figures 4I–4L. All three lines yielded two major classes of mosaics. Animals in one class of mosaics expressed *str-2*::GFP in the wild-type cell but not in the gain-of-function, RFP+ cell, and animals in the second class did not express *str-2*::GFP in either cell. These are the classes expected if *unc-43* were acting to execute the AWC^{OFF} cell fate, but not to coordinate the fates of the two AWC cells via cell interaction (Figure 3C). Statistical analysis for all three lines was consistent with the model that *unc-43* acts only to execute the AWC^{ON} cell fate decision (Table 1). The results of mosaic analysis with both gain-of-function and loss-of function *unc-43* thus support the model that *unc-43* acts cell autonomously to execute the AWC^{OFF} fate and does not contribute to the specification of the AWC^{ON} fate.

nsy-1 Executes the AWC^{OFF} Cell Fate, but May Also Play a Minor Role in Coordinating the Fates of the Two AWC Neurons

Using the approach described above for *unc-43*, we performed mosaic analysis experiments with a *nsy-1* loss-of-function mutant and a *nsy-1* gain-of-function transgene. The results of these experiments are reported in Table 1 and Figure 4.

Three transgenic lines were used in the *nsy-1* loss-of-function mosaic analysis. In all lines, two major classes of mosaics were observed (Table 1, Figures 4E–4H): in one class, only the mutant cell expressed *str-2*::GFP, and in the other class, both cells expressed *str-2*::GFP. These are the same mosaic classes observed in the *unc-43* loss-of-function mosaic analysis and are the two classes expected for a gene involved only in executing the AWC^{OFF} fate (Figure 3B). Statistical analysis of the results, however, revealed that these mosaics did not fit the model that *nsy-1* acts exclusively to execute the AWC^{OFF} fate (Table 1). Two of three lines generated significantly more mosaic animals than expected in the class that expressed *str-2*::GFP in the *nsy-1* mutant AWC cell but not the wild-type AWC cell. This class of mosaics would predominate if *nsy-1* played a role in cell interaction and feedback. The results for *nsy-1(lf)* mosaics therefore support a model in which *nsy-1* acts mostly cell autonomously to execute the AWC^{OFF} cell fate, but may also have a minor influence on cell interaction and feedback in a separate, *unc-43*-independent role.

Mosaic analysis was also performed with five *nsy-1* gain-of-function lines. Again, the two major classes of mosaics expected in the execution model were observed (Table 1, Figures 4M–4P). Two of the lines exhibited approximately equal numbers of the two major classes of mosaics (lines a and c), two of the lines were slightly enriched in mosaics that did not express *str-2*::GFP at all (lines d and e), and one of the lines was strikingly enriched in this class of mosaics (line b). Although all of these results are closer to the execution model than the cell interaction and feedback model, lines a and c statistically fit this model, but lines b, d, and e did not (Table 1). In lines b, d, and e, the *nsy-1(gf)* cell appeared to act as a weak dominant-negative in the cell interaction, not as a gain-of-function. The disruption of the N terminus of *nsy-1*, which is missing in NSY-1(GF), may create a mixed gain-of-function and dominant-negative *nsy-1* allele. The simplest interpretation of the mosaic analyses for *nsy-1(lf)* and *nsy-1(gf)* is that *nsy-1* plays a predominately cell-autonomous role downstream of *unc-43* to execute the AWC^{OFF} cell fate, but also has the potential to play a nonessential, minor role in coordinating the fates of the two AWC cells.

Discussion

The CaMKII UNC-43 Activates the MAPKKK ASK1/NSY-1 to Regulate AWC Cell Fate

nsy-1, a gene involved in determining asymmetric cell fates in the AWC olfactory neurons, encodes the likely ortholog of the human MAPKKK ASK1 (Ichijo et al., 1997). Our genetic results predict that calcium signaling through a voltage-gated calcium channel and the *C.*

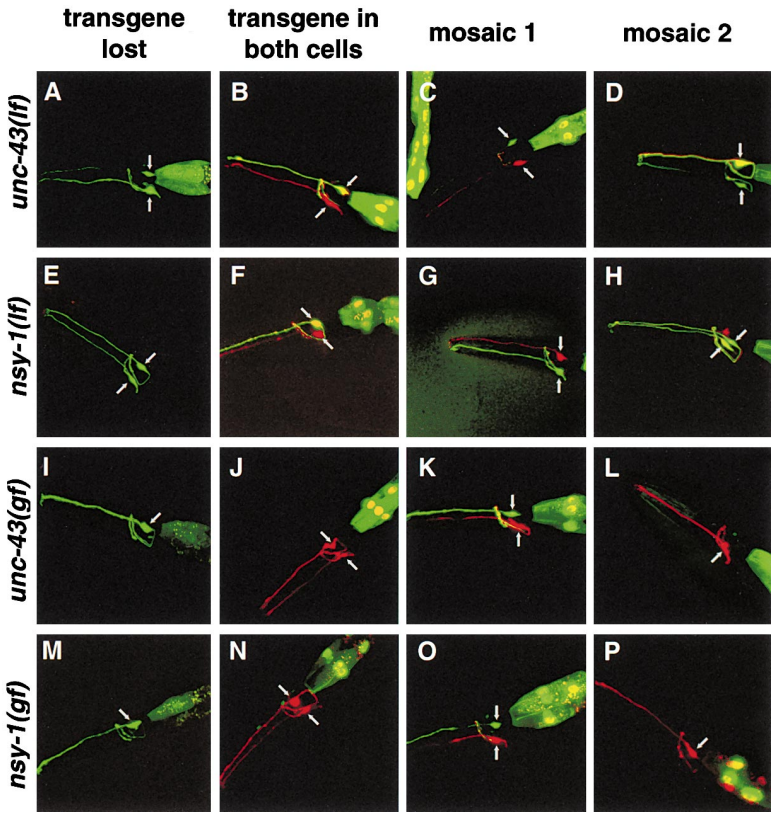

Figure 4. *str-2::GFP* Expression in Control and Mosaic Animals

Confocal projections of animals expressing a stable, integrated *str-2*::GFP transgene and an unstable transgenic array with a test plasmid and *odr-1*::RFP. (A–D) *odr-3*::UNC-43 plasmid in an *unc-43(n1186lf)* strain, (E–H) *odr-3*::NSY-1 plasmid in a *nsy-1(ky397)* strain, (I–L) *odr-3*::UNC-43(GF) plasmid in a wild-type strain, (M–P) *odr-3*::NSY-1(GF) plasmid in a wild-type strain. *str-2*::GFP fluorescence was false-colored green and *odr-1*::RFP fluorescence was false-colored red. Overlap between red and green appears yellow. AWC cells are indicated by arrows. (A, E, I, and M) Control animals that lost the array from both AWC cells. (A and E) 2 AWC^{ON} phenotype when wild-type rescuing transgenes were lost from *nsy-1(lf)* and *unc-43(lf)* strains. (I and M) Wild-type phenotype (1 AWC^{ON}/1 AWC^{OFF}) when *nsy-1(gf)* and *unc-43(gf)* transgenes were lost from a wild-type strain. (B, F, J, and N) Control animals expressing the array in both AWC cells. (B and F) In *nsy-1(lf)* and *unc-43(lf)* lines, the transgene rescued asymmetric expression of *str-2*::GFP (1 AWC^{ON}/1 AWC^{OFF}). (J and N) In *nsy-1(gf)* and *unc-43(gf)* lines, the transgene caused a 2 AWC^{OFF} phenotype. Mosaic animals: (C and G) In some *nsy-1(lf)* and *unc-43(lf)* AWC mosaics the wild-type RFP+ cell was AWC^{OFF}, whereas the mutant RFP− cell was AWC^{ON}. (D and H) In some *nsy-1(lf)* and *unc-43(lf)* mosaics, both the wild-type and mutant cells were AWC^{ON}. (K and O) In some *nsy-1(gf)* and *unc-43(gf)* mosaics, the activated RFP+ cell was AWC^{OFF}, and the wild-type RFP− cell was AWC^{ON}. (L and P) In some *nsy-1(gf)* and *unc-43(gf)* mosaics both the wild-type and mutant cells were AWC^{OFF}. Dorsal is up and anterior is left in all panels. Fluorescence posterior to the head is gut autofluorescence or gut expression of the transgene marker *elt-2*::GFP (see Experimental Procedures). In (H) and (J), *odr-1*::RFP is also visible in AWB, a smaller cell.

elegans CaMKII UNC-43 activates the NSY-1 MAPKKK. *nsy-1* and *unc-43* mutants have identical *str-2*::GFP expression phenotypes, and both can act as switches in the establishment of AWC asymmetry. Mosaic analysis demonstrates that both act in the AWC^{OFF} cell to repress *str-2* expression. Epistasis analysis places *nsy-1* downstream of *unc-43*, and the UNC-43 and NSY-1 proteins associate in heterologous cells, suggesting that their interaction may be direct. Indeed, the NSY-1/ASK1 MAPKKK pathway is activated by CaMKII in both *C. elegans* and mammalian cultured cells, supporting the predictions of the genetic model (M. Tanaka-Hino et al., submitted; K. Takeda et al., submitted).

The link between CaMKII and NSY-1/ASK1 was unanticipated. CaMKII was previously shown to activate ERK, but not p38/JNK MAP kinases (e.g., Watt and Storm, 2001); conversely, several different activators, but not CaMKII, were previously linked to ASK1. In mammalian cells, ASK1 promotes apoptosis in response to tumor necrosis factor-α and activation of the Fas death receptor (Chang et al., 1998; Ichijo et al., 1997). Tumor necrosis factor activation of ASK1 is mediated by the adaptor protein TRAF2, and Fas activation of ASK1 is mediated by the Daxx adaptor (Chang et al., 1998; Nishitoh et al., 1998). ASK1 may also be involved in G protein–coupled receptor signaling through an interaction with β-arrestin (Berestetskaya et al., 1998; McDonald et al., 2000). It does not always promote cell death; in PC12 cells, ASK1 promotes neuronal differentiation (Takeda et al., 2000).

As predicted by its similarity to ASK1, NSY-1 expression can stimulate the phosphorylation of the MAPKK MEK6 and p38 MAPK in heterologous cells. The *C. elegans* genome contains at least three MAPKKKs, ten MAPKKs, and fourteen MAPKs (five ERK class, five JNK class, three p38 class, and one NLK class) (Plowman et al., 1999). Although several candidates have been tested (data not shown), we have not yet identified a *C. elegans* MAPK that affects AWC asymmetry.

The ERK, JNK, and p38 MAP kinases are related to one another by sequence, but different classes are regulated by different inputs and have distinct outputs. Many cell fate decisions are controlled by ERK MAP kinase signaling cassettes, particularly downstream of receptor tyrosine kinase/ras signaling pathways (reviewed in Garrington and Johnson, 1999). Their intrinsic ultrasensitivity and reinforcing feedback loops make MAPK pathways well-suited to all-or-none developmental fate decisions (Ferrell, 1996). The JNK and p38 MAPKs respond to environmental stresses (such as ultraviolet light) and inflammatory cytokines, and regulate apoptosis and nonmitogenic inflammatory responses. JNK also functions in some developmental decisions, including dorsal closure and tissue polarity in *Drosophila* (Noselli, 1998; reviewed in Davis, 2000). The functional divi-

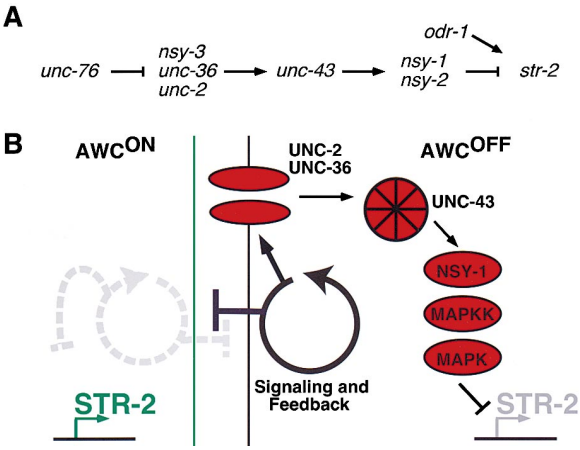

Figure 5. A Model for Execution of the AWC^{OFF} Fate

(A) Epistasis relationships of *nsy* mutants.

(B) In the AWC^{OFF} cell, calcium influx through the UNC-2/UNC-36 calcium channel activates the calcium/calmodulin-dependent kinase UNC-43, which in turn activates the NSY-1 MAPKKK. Activation of the NSY-1 MAPK cascade leads to repression of *str-2* transcription. The CaMKII/NSY-1 pathway is less active in the AWC^{ON} cell, allowing expression of *str-2*. By analogy to Notch, the fates of the two cells are initially specified by a cell interaction that may use feedback to amplify differences between the AWC cells. This pathway acts upstream of the calcium/CaMKII/NSY-1 AWC^{OFF} execution pathway.

sion between MAP kinases is conserved in yeast: the KSS1/FUS3 ERK proteins act in differentiation (mating and filamentous growth), whereas the HOG1 p38 kinase acts in the osmotic stress response. The AWC asymmetry decision represents an unusual case of the p38/JNK pathway acting in a cell fate decision. In addition, AWC asymmetry has the unusual property of using calcium signaling to control cell fate. Because the developing AWC neurons are relatively mature and have sent out axons by the time the decision is made, they may have access to the calcium channels that are more typically involved in neuronal signaling. In one scenario, the AWC cell fate decision may be recruiting a stress response pathway to a developmental decision.

The broad expression pattern of *nsy-1* suggests that it has other functions in addition to its role in controlling *str-2* asymmetry, and might regulate other cell fates. In addition, since calcium entry contributes to stress following prolonged excitation of neurons, the same pathway may contribute to physiological detection of stress in other circumstances. For example, since ASK1 can act as an activator of cell death (Ichijo et al., 1997; Berestetskaya et al., 1998; Chang et al., 1998), we speculate that CaMKII and ASK1 may play a role in excitotoxic cell death in response to calcium influx. Calcium signals can also affect cell migration, axon guidance, and neuronal plasticity. Even among kinases, there are numerous targets for calcium signals: CaMKII activates the ERK MAP kinase in several cell types, including mammalian olfactory neurons (Watt and Storm, 2001), and the ras/ERK pathway responds to sensory activity in *C. elegans* olfactory neurons (Hirotsu et al., 2000). JNK can be activated by a CaMKIV pathway in PC12 cells (Enslen et al., 1996). The UNC-43/CaMKII-NSY-1/ASK1 pathway could act in a variety of calcium-dependent processes, either alone or in combination with other ERK and JNK pathways.

UNC-43/CaMKII and NSY-1/ASK1 Execute the AWC^{OFF} Fate

UNC-43/CaMKII and NSY-1/ASK1 have central roles in a cell interaction that determines cell fates in the olfactory system of *C. elegans* (Troemel et al., 1999). Although most neurons in *C. elegans* exist as bilaterally symmetric, morphologically similar pairs, the two AWC olfactory neurons interact with each other to allow AWCL and AWCR to adopt distinct fates. The stochastic and coordinated interaction that determines AWC asymmetry is reminiscent of lateral signaling, a process that allows two initially equivalent cells to coordinate their fates so that each adopts a distinct identity. The only well-characterized molecular pathway that accomplishes lateral signaling is mediated by Notch family receptors (Kimble and Simpson, 1997). In lateral signaling interactions mediated by Notch, ablating one of the interacting cells causes the remaining cell to adopt a default fate (e.g., Kimble, 1981). Similarly, ablating one of the two AWC cells causes the remaining cell to adopt the AWC^{OFF} fate (Troemel et al., 1999). However, several features of the AWC lateral interaction are not typical for Notch signaling: the signaling between the two AWC neurons is mediated by calcium and a MAPK pathway, and occurs in relatively mature neurons whose axons have made contact with each other. In addition, unlike Notch lateral signaling, UNC-43/NSY-1 signaling primarily affects execution of the AWC^{OFF} fate and not feedback between the AWC neurons.

unc-43 and *nsy-1* act in the AWC neuron pair to control the asymmetric expression of *str-2*::GFP. Expressing either *nsy-1* or *unc-43* in both AWC cells restored asymmetric cell fates in *nsy-1* and *unc-43* mutants, demonstrating that it is not the asymmetric expression of these genes but rather asymmetric activity that controls AWC cell fates. A signal from the AWC^{OFF} cell is required for the AWC^{ON} fate, but *unc-43* and *nsy-1* are required for the AWC^{OFF} fate; their activities may be repressed by the initial signal.

Genetic mosaic analysis was used to ask whether *unc-43* and *nsy-1* are required in a strictly cell autonomous manner to execute the AWC^{OFF} cell fate, or whether they also play roles in coordinating the two cell fates. The mosaic strategy and cell interaction model were based on the AC/VU lateral signaling decision that occurs between two cells in the *C. elegans* hermaphrodite gonad, Z1.ppp and Z4.aaa (Kimble, 1981). Z1.ppp and Z4.aaa make a stochastic, coordinated decision that allows one cell to adopt an anchor cell (AC) fate and the other cell to adopt a ventral uterine precursor cell (VU) fate. This interaction requires the Notch family receptor *lin-12* (Greenwald et al., 1983). Seydoux and Greenwald (1989) used genetic mosaic analysis to show that *lin-12* activity is required in the VU cell to allow it to receive an inducing signal from the AC cell. If *lin-12* was mutant in one of the two AC/VU cells, the mutant cell always adopted the AC fate and the wild-type cell always adopted the VU fate. Because *lin-12* is involved in the feedback loop between AC and VU, loss of *lin-12*

activity in one cell had a nonautonomous effect that forced the other cell to become VU. By analogy, we reasoned that if *unc-43* and *nsy-1* are involved in a feedback loop in the AWC cell fate decision, the loss of *unc-43* and *nsy-1* activity in one AWC neuron would result in mosaic animals with one AWC^{OFF} (wild-type) and one AWC^{ON} (mutant) cell every time. A different result is expected if these genes act to execute the AWC^{OFF} cell fate. The execution model predicts that half of the mosaic animals would have two AWC^{ON} cells. The mutant cell will always adopt the AWC^{ON} fate, whereas the wild-type cell will take on the AWC^{ON} and AWC^{OFF} fates with equal frequency.

Genetic mosaic analyses with *unc-43* gain-of-function and loss-of-function mutants fit the prediction for a strictly cell-autonomous gene that executes the AWC^{OFF} cell fate in one cell. Loss-of-function and gain-of-function mosaics with *nsy-1* were also mostly consistent with the execution model: the presence of two classes of *nsy-1(lf)* and *nsy-1(gf)* mosaics supports the idea that *nsy-1* functions mainly to execute the AWC^{OFF} cell fate cell autonomously. However, the class of mosaics with one AWC^{ON} (mutant) and one AWC^{OFF} (wild-type) neuron was more prevalent in *nsy-1(lf)* mosaics, suggesting that *nsy-1* has a minor cell nonautonomous effect on AWC fate.

Our results suggest a model for the execution of the AWC^{OFF} cell fate (Figure 5). An initial lateral signaling interaction between the two AWC cells defines one cell as AWC^{ON} and the other as AWC^{OFF}. In the cell defined as AWC^{OFF}, calcium influx through a voltage-gated calcium channel (UNC-2 and UNC-36) activates the calcium-calmodulin dependent kinase UNC-43, which in turn activates the MAPKKK NSY-1. Activation of the MAPKKK pathway represses *str-2* transcription in the AWC^{OFF} cell. In contrast with signaling molecules of Notch pathways, the CaMKII/NSY-1 signaling cassette is not an essential component of lateral signaling and feedback. The genes that participate in the initial AWC cell interaction are not known. One candidate for a molecule involved in this lateral signaling pathway is *nsy-3*, which is genetically upstream of or parallel to the CaMKII *unc-43*. *nsy-2* is a candidate to act at a downstream step in execution, since like *nsy-1* it is epistatic to *unc-43*. Our results, coupled with the observation that NSY-1 and UNC-43 have well-conserved mammalian homologs, raise the possibility that the calcium-to-MAPK signaling cassette used in AWC cell fate determination may be used for cell fate diversification in other animals.

Experimental Procedures

Strains

Wild-type strains were *C. elegans* variety Bristol, strain N2. Unless otherwise noted, strains contained the integrated *str-2::*GFP transgene *kyIs140 (I)* (Troemel et al., 1999). Strains were maintained by standard methods (Brenner, 1974).

Mapping and Cloning *nsy-1*

nsy-1(ky397) was mapped on LGII between *stP196* and *stP36*, two Tc1 transposable element polymorphisms in the DP13 strain (Williams, 1995). The deficiencies *ccDf2* and *maDf4* failed to complement *nsy-1*, whereas the deficiencies *ccDf11* and *mnDf30* complemented *nsy-1*. Cosmid clones representing the *nsy-1* genomic region were injected into *nsy-1(ky397)* at a concentration of ~10 μg/ml each. The cosmid C51A9 (overlapping F59A6) rescued asymmetric expression of *str-2*::GFP in three of four transgenic lines (all rescued lines were ≥ 91% 1 AWC^{ON}/1 AWC^{OFF}). A 13.1 kb SacI deletion fragment of C51A9 containing only the full open reading frame for the F59A6.1 gene rescued *str-2*::GFP asymmetry in *nsy-1(ky397)* in four of four lines (all lines ≥ 80% 1 AWC^{ON}/1 AWC^{OFF}). A subclone with the F59A6.1 gene and 3.8 kb of upstream sequence partially rescued *str-2*::GFP asymmetry in only one of eight transgenic lines (the one rescued line was 50% 1 AWC^{ON}/1 AWC^{OFF}, 50% 2 AWC^{ON}). The *nsy-1* (F59A6.1) genomic coding region in *ky397*, *ky400*, and *ky542* was amplified by PCR in several pieces and PCR products were directly sequenced.

Plasmid Construction

nsy-1::GFP

A region including ~10 kb of sequence upstream of the *nsy-1* gene was amplified by PCR and subcloned into the pPD95.77 vector.

nsy-1 *and* nsy-1(gf) *cDNA Construction*

A full-length *nsy-1* cDNA was assembled from the EST yk321g3 (a gift of Y. Kohara) and a partial cDNA amplified by PCR from a *C. elegans* cDNA library (Kawasaki et al., 1999). To make a *nsy-1(gf)* cDNA, the region corresponding to the first 640 amino acids of the cDNA was deleted by PCR.

odr-3*::NSY-1 and* odr-3*::NSY-1(GF)*

The full-length *nsy-1* cDNA and the *nsy-1(gf)* were subcloned into a vector with an EcoRV fragment of the *odr-3* promoter (Roayaie et al., 1998).

odr-3*::UNC-43 and* odr-3*::UNC-43(GF)*

An *unc-43* cDNA (KP354) and an *unc-43(gf)* cDNA (T284D; KP421) were provided generously by Josh Kaplan (Rongo and Kaplan, 1999). Both were subcloned into the *odr-3* promoter vector (see above).

odr-1::RFP

GFP was replaced by RFP (dsRed, Clontech) in an *odr-1*::GFP plasmid (L'Etoile and Bargmann, 2000).

Further details of plasmid construction are available upon request.

Germ-Line Transformation

Transgenic strains were made as previously described (Mello and Fire, 1995). *odr-1*::RFP, *elt-2::GFP*, and cosmids were injected at 10–15 μg/ml; all other plasmids were injected at 50 μg/ml. For rescue experiments, the dominant pRF4 *rol-6(su1006)* coinjection marker was injected with test plasmids into a *nsy-1(ky397)* strain containing a *str-2::*GFP transgene (*kyIs140*). *nsy-1::*GFP expression was examined by injection of test plasmids and the *lin-15* plasmid pJM23 into *lin-15(n765ts)* strains. For mosaic animals, an *elt-2*::GFP injection marker (a gift of J. McGhee), which causes intense fluorescence in the gut, was injected with test plasmids. Transgenes were maintained by picking Rol animals, nonMuv animals, or animals expressing *elt-2*::GFP.

Biochemistry

Immunoprecipitation from mammalian cells, in vitro kinase assays, and immunoblotting were carried out as described (Kawasaki et al., 1999). Mammalian expression vectors were transfected into HEK 293 cells using the calcium phosphate precipitation method. Proteins from the cell lysates were immunoprecipitated with anti-T7 antibodies (Novagen). For kinase assays, aliquots of immunoprecipitates were incubated with bacterially expressed His-MKK6 in kinase buffer at 25°C for 2 min. Samples were analyzed by SDS-PAGE and autoradiography. The immunoprecipitates and aliquots of total lysates were analyzed by immunoblotting and visualized by Enhanced Chemiluminesence (ECL) Western Blotting System (Amersham).

Genetic Mosaic Analysis

Mosaic analysis was performed according to the general method described by Herman (1984). Animals of the appropriate background (see Table 1) were injected with a mix of transgenes including *elt-2*::GFP, *odr-1*::RFP and either *odr-3*::UNC-43, *odr-3*::NSY-1, *odr-3*::UNC-43(GF), or *odr-3*::NSY-1(GF). Transgenic lines were passaged for ten generations to allow the transgenes to stabilize before screening for mosaics. The presence of the array could be scored

in the AWC and AWB neurons, which express the *odr-1::*RFP transgene.

Since the *odr-3* promoter is expressed in both AWB and AWC, we asked whether AWB has a role in regulating AWC cell fate. Control animals were generated that lost the array in both AWC neurons but maintained expression in AWB neurons. The results of these experiments excluded a function for *unc-43* or *nsy-1* in AWB. Results for transgenes in which neither AWC neuron, but one or both AWB neurons expressed RFP: For *odr-3::*UNC-43 rescue of *unc-43(n1186)*, 0/8 animals with one AWB+ and 0/6 animals with two AWB+ neurons were rescued; for *odr-3::*NSY-1 rescue of *nsy-1(n397)*, 1/30 animals with one AWB+ and 0/1 animals with two AWB+ neurons were rescued; for *odr-3::*UNC-43(GF) introduced into wild-type, 0/11 animals with one AWB+ and 0/7 animals with two AWB+ neurons exhibited the gain-of-function phenotype; for *odr-3::*NSY-1(GF) introduced into wild-type, 0/30 animals with one AWB+ and 0/17 animals with two AWB+ neurons exhibited the gain-of-function phenotype.

To dissect the circuitry of signaling between the two AWC cells, mosaic animals that lost the array in one AWC cell (1 RFP+ and 1 RFP− AWC cell) were scored for each line. Internal controls were generated by scoring animals that lost the array in both AWC neurons (RFP−) and animals that retained the array in both AWC neurons (RFP+). For *unc-43(lf)* and *nsy-1(lf)* analysis, animals that lost the wild-type transgene from both AWC cells (2 RFP−) expressed *str-2*::GFP in both cells (all lines $\geq$ 97% 2 AWC^{ON}, n $\geq$ 311). For *unc-43(gf)* and *nsy-1(gf)* analysis, animals that lost the gain-of-function transgene from both AWC cells (2 RFP−), expressed *str-2*::GFP in one AWC cell (all lines $\geq$ 98% 1 AWC^{ON}/1 AWC^{OFF}, n $\geq$ 50).

Statistical Analysis

Data from all lines were analyzed with χ^2 tests to determine whether *unc-43* or *nsy-1* fit models that they act in cell interaction and feedback or solely in the execution of the AWC^{OFF} fate (see Table 1 for results of these analyses). Models for statistical analyses were generated from results for internal controls expressing the transgene in both AWC cells (2 RFP+). For example, when the *odr-3*::UNC-43 transgene was expressed in both AWC cells in the *unc-43(lf)* mosaic line "a", 16% of the animals had a 2 AWC^{OFF} (gain-of-function) phenotype, 55% of the animals had a 1 AWC^{ON}/1 AWC^{OFF} (rescued) phenotype, and 29% of the animals had a 2 AWC^{ON} (mutant) phenotype. The model that *unc-43* acts in execution was generated as follows: In all cases, the mutant RFP− cell was predicted to be AWC^{ON}; this prediction was correct in >90% of animals. The anomalous cases in which the RFP− cell was AWC^{OFF} (<10% of animals) were not included in statistical analysis. Sixteen percent of mosaics were expected to have a gain-of-function transgene in the RFP+ cell and were thus expected to have a transgenic cell that was AWC^{OFF} and a nontransgenic (mutant) cell that was AWC^{ON}. Fifty-five percent of mosaics were expected to have a "rescued" RFP+ cell that had an equal chance of being AWC^{ON} or AWC^{OFF}, so, in our model, half of this percentage (27.5%) was expected to have a 1 AWC^{ON} (mutant)/1 AWC^{OFF} (rescued cell) phenotype and the other 27.5% was expected to have a 2 AWC^{ON} phenotype. In 29% of controls, the transgene did not rescue the *unc-43* mutant phenotype, so the corresponding 29% of mosaics were expected to have a 2 AWC^{ON} phenotype. Thus, our model predicted that 43.5% (16 + 27.5) of mosaics would have an AWC^{OFF} (RFP+) cell and an AWC^{ON} (RFP−) cell, and 56.5% (27.5 + 29) would have 2 AWC^{ON} cells. For the cell interaction model, all 55% of the "rescued" RFP+ cells were expected to be AWC^{OFF} in the presence of a mutant AWC^{ON} cell, predicting 71% (16 + 55) 1 AWC^{ON}/1 AWC^{OFF} animals and 29% 2 AWC^{ON} animals. These percentages were multiplied by the number of mosaics generated in the experiment (in this case 71), and the resulting numbers were compared by χ^2 analysis with the actual numbers of mosaics observed. Analogous logic was applied to generate models for both loss-of-function and gain-of-function mosaic experiments with *unc-43* and *nsy-1*.

One possible explanation for the skewed proportions of mosaics in *nsy-1(lf)* mosaics is that the *odr-3* promoter is expressed at a low level in AWC precursors, and that even if expression is lost in AWC itself (as determined by lack of RFP expression), perdurance of the NSY-1 protein was able to rescue *str-2::GFP* asymmetry. This model could explain the existence of a small number of anomalous animals in a third class of mutants (wild-type (RFP+) AWC^{ON}/mutant (RFP−) AWC^{OFF}). We tested this possibility statistically by removing this anomalous class from our analysis, as well as an equal number of animals from the overrepresented class (wild-type (RFP+) AWC^{OFF}/mutant (RFP−) AWC^{ON}). Following this analysis, *nsy-1(lf)* lines (a) and (b) were still statistically different from the pure execution model. Therefore perdurance could account for some, but not all, of the nonautonomous effects of *nsy-1.*

Acknowledgments

We are grateful to Mike Springer for insightful comments on statistical interpretation, Oliver Hobert, Amanda Kahn, Miri VanHoven, and Paul Wes for helpful discussions and comments on the manuscript, and Jason Much and Hai Nguyen for excellent technical support. We thank Lisa Williams for examining cell migrations in *nsy-1* and *unc-43* mutants, Maria Gallegos for help with microscopy, Kang Shen for RFP PCR product, Alan Coulson and the Sanger Center for cosmids, Yuji Kohara for EST clones, Andy Fire for *C. elegans* vectors, Josh Kaplan for the *unc-43* cDNAs, and Jim McGhee for *elt-2*::GFP. This work was supported by the National Institutes of Health (C. I. B) and special grants from CREST, Advanced Research on Cancer from the Ministry of Education, Culture and Science of Japan, the Uehara Memorial Foundation, and the Daiko Foundation (to K. M.). A. S. is a Howard Hughes Medical Institute predoctoral fellow and C. I. B. is an Investigator of the Howard Hughes Medical Institute.

Received December, 2000; revised March 22, 2001.

References

Berestetskaya, Y.V., Faure, M.P., Ichijo, H., and Voyno-Yasenetskaya, T.A. (1998). Regulation of apoptosis by alpha-subunits of G12 and G13 proteins via apoptosis signal-regulating kinase-1. J. Biol. Chem. *273*, 27816–27823.

Brenner, S. (1974). The genetics of *Caenorhabditis elegans*. Genetics *77*, 71–94.

Chalfie, M., Tu, Y., Euskirchen, G., Ward, W.W., and Prasher, D.C. (1994). Green fluorescent protein as a marker for gene expression. Science *263*, 802–805.

Chang, H.Y., Nishitoh, H., Yang, X., Ichijo, H., and Baltimore, D. (1998). Activation of apoptosis signal-regulating kinase 1 (ASK1) by the adapter protein Daxx. Science *281*, 1860–1863.

Davis, R.J. (2000). Signal transduction by the JNK group of MAP kinases. Cell *103*, 239–252.

Enslen, H., Tokumitsu, H., Stork, P.J., Davis, R.J., and Soderling, T.R. (1996). Regulation of mitogen-activated protein kinases by a calcium/calmodulin-dependent protein kinase cascade. Proc. Natl. Acad. Sci. USA *93*, 10803–10808.

Ferrell, J.E., Jr. (1996). Tripping the switch fantastic: how a protein kinase cascade can convert graded inputs into switch-like outputs. Trends Biochem. Sci. *21*, 460–466.

Garrington, T.P., and Johnson, G.L. (1999). Organization and regulation of mitogen-activated protein kinase signaling pathways. Curr. Opin. Cell Biol. *11*, 211–218.

Greenwald, I.S., Sternberg, P.W., and Horvitz, H.R. (1983). The *lin-12* locus specifies cell fates in *Caenorhabditis elegans*. Cell *34*, 435–444.

Herman, R.K. (1984). Analysis of genetic mosaics of the nematode *Caneorhabditis elegans*. Genetics *108*, 165–180.

Hirotsu, T., Saeki, S., Yamamoto, M., and Iino, Y. (2000). The Ras-MAPK pathway is important for olfaction in *Caenorhabditis elegans*. Nature *404*, 289–293.

Ichijo, H., Nishida, E., Irie, K., ten Dijke, P., Saitoh, M., Moriguchi, T., Takagi, M., Matsumoto, K., Miyazono, K., and Gotoh, Y. (1997). Induction of apoptosis by ASK1, a mammalian MAPKKK that activates SAPK/JNK and p38 signaling pathways. Science *275*, 90–94.

Kawasaki, M., Hisamoto, N., Iino, Y., Yamamoto, M., Ninomiya-Tsuji, J., and Matsumoto, K. (1999). A *Caenorhabditis elegans* JNK signal transduction pathway regulates coordinated movement via type-D GABAergic motor neurons. EMBO J. *18*, 3604–3615.

Kimble, J. (1981). Alterations in cell lineage following laser ablation of cells in the somatic gonad of *Caenorhabditis elegans*. Dev. Biol. *87*, 286–300.

Kimble, J., and Simpson, P. (1997). The LIN-12/Notch signaling pathway and its regulation. Annu. Rev. Cell Dev. Biol. *13*, 333–361.

L'Etoile, N.D., and Bargmann, C.I. (2000). Olfaction and odor discrimination are mediated by the *C. elegans* guanylyl cyclase ODR-1. Neuron *25*, 575–586.

Lee, R.Y., Lobel, L., Hengartner, M., Horvitz, H.R., and Avery, L. (1997). Mutations in the alpha1 subunit of an L-type voltage-activated Ca2+ channel cause myotonia in *Caenorhabditis elegans*. EMBO J. *16*, 6066–6076.

McDonald, P.H., Chow, C.W., Miller, W.E., Laporte, S.A., Field, M.E., Lin, F.T., Davis, R.J., and Lefkowitz, R.J. (2000). beta-Arrestin 2: A receptor-regulated MAPK scaffold for the activation of JNK3. Science *290*, 1574–1577.

Mello, C., and Fire, A. (1995). DNA transformation. Methods Cell Biol. *48*, 451–482.

Nishitoh, H., Saitoh, M., Mochida, Y., Takeda, K., Nakano, H., Rothe, M., Miyazono, K., and Ichijo, H. (1998). ASK1 is essential for JNK/SAPK activation by TRAF2. Mol. Cell *2*, 389–395.

Noselli, S. (1998). JNK signaling and morphogenesis in *Drosophila*. Trends Genet. *14*, 33–38.

Plowman, G.D., Sudarsanam, S., Bingham, J., Whyte, D., and Hunter, T. (1999). The protein kinases of *Caenorhabditis elegans*: a model for signal transduction in multicellular organisms. Proc. Natl. Acad. Sci. USA *96*, 13603–13610.

Reiner, D.J., Newton, E.M., Tian, H., and Thomas, J.H. (1999). Diverse behavioural defects caused by mutations in *Caenorhabditis elegans unc-43* CaM kinase II. Nature *402*, 199–203.

Roayaie, K., Crump, J.G., Sagasti, A., and Bargmann, C.I. (1998). The G alpha protein ODR-3 mediates olfactory and nociceptive function and controls cilium morphogenesis in *C. elegans* olfactory neurons. Neuron *20*, 55–67.

Rongo, C., and Kaplan, J.M. (1999). CaMKII regulates the density of central glutamatergic synapses *in vivo*. Nature *402*, 195–199.

Saitoh, M., Nishitoh, H., Fujii, M., Takeda, K., Tobiume, K., Sawada, Y., Kawabata, M., Miyazono, K., and Ichijo, H. (1998). Mammalian thioredoxin is a direct inhibitor of apoptosis signal-regulating kinase (ASK) 1. EMBO J. *17*, 2596–2606.

Schafer, W.R., and Kenyon, C.J. (1995). A calcium-channel homologue required for adaptation to dopamine and serotonin in *Caenorhabditis elegans*. Nature *375*, 73–78.

Seydoux, G., and Greenwald, I. (1989). Cell autonomy of *lin-12* function in a cell fate decision in *C. elegans*. Cell *57*, 1237–1245.

Takeda, K., Hatai, T., Hamazaki, T.S., Nishitoh, H., Saitoh, M., and Ichijo, H. (2000). Apoptosis signal-regulating kinase 1 (ASK1) induces neuronal differentiation and survival of PC12 cells. J. Biol. Chem. *275*, 9805–9813.

Troemel, E.R., Sagasti, A., and Bargmann, C.I. (1999). Lateral signaling mediated by axon contact and calcium entry regulates asymmetric odorant receptor expression in *C. elegans*. Cell *99*, 387–398.

Watt, W.C., and Storm, D.R. (2001). Odorants stimulate the Erk/MAP kinase pathway and activate CRE-mediated transcription in olfactory sensory neurons. J. Biol. Chem. *276*, 2047–2052.

Wes, P.D., and Bargmann, C.I. (2001). C. elegans odour discrimination requires asymmetric diversity in olfactory neurons. Nature *410*, 698–701.

White, J.G., Southgate, E., Thomson, J.N., and Brenner, S. (1986). The structure of the nervous system of the nematode *Caenorhabditis elegans*. Phil. Trans. R. Soc. Lond. B *314*, 1–340.

Williams, B.D. (1995). Genetic mapping with polymorphic sequence-tagged sites. Methods Cell Biol. *48*, 81–96.

Yu, S., Avery, L., Baude, E., and Garbers, D.L. (1997). Guanylyl cyclase expression in specific sensory neurons: a new family of chemosensory receptors. Proc. Natl. Acad. Sci. USA *94* 3384–3387.